Fabrication of ferromagnetic rolled-up microtubes for magnetic sensors on fluids

IOP PUBLISHING JOURNAL OF PHYSICS D: APPLIED PHYSICS

J. Phys. D: Appl. Phys. **42** (2009) 055001 (8pp) doi:10.1088/0022-3727/42/5/055001

Fabrication of ferromagnetic rolled-up microtubes for magnetic sensors on fluids

Esteban Bermúdez Ureña[1,4], Yongfeng Mei[1], Emica Coric[1], Denys Makarov[2], Manfred Albrecht[3] and Oliver G Schmidt[1]

[1] Institute for Integrative Nanosciences, IFW Dresden, Helmholtzstrasse 20, D-01069 Dresden, Germany
[2] Department of Physics, University of Konstanz, Universitätstrasse 10, D-78457 Konstanz, Germany
[3] Chemnitz University of Technology, Institute of Physics, Reichenhainer Str. 70, D-09107 Chemnitz, Germany

E-mail: ebermudez85@gmail.com

Received 31 October 2008, in final form 11 December 2008
Published 5 February 2009
Online at stacks.iop.org/JPhysD/42/055001

Abstract

Ferromagnetic microtubes are fabricated by the deterministic release of thin magnetic films from a photoresist sacrificial layer. Crucial steps towards the fabrication of well positioned and uniform single rolled-up tubes are presented, where the final and main approach consists of releasing angled deposited magnetic films by dissolving an underlying patterned photoresist layer. Microtubes from soft magnetic $Ni_{80}Fe_{20}$ films and Co/Pt multilayer stacks with perpendicular magnetic anisotropy are obtained with predefined lengths and diameters down to 1.5 μm. The nonlinear rotational dynamics of the tubes in viscous fluids is investigated. Sensitivities to viscosity variations for tubes with different lengths are observed and suggest their potential application as single sensing probes in a wide range of viscosities. Moreover, the variation in the characteristic critical frequency of the rotational motion for chains of magnetically coupled microtubes agrees with the expected changes in the theoretical shape factor of cylindrical particles. Evidence of tube remagnetization during the rotation opens the way to investigate properties such as the switching fields of individual tubes.

(Some figures in this article are in colour only in the electronic version)

1. Introduction

The search for new types of magnetic structures in the micro- and nanoscale has become an exciting area of interest, from new concepts and geometries for magnetic sensors [1] and recording media [2] to polyfunctional particles for biomedical applications such as organism targeting and drug delivery [3]. Tubular magnetic structures are highly attractive for biomedical applications due to their low density and the possibility to manipulate them by external fields. The increased surface area, with the inner and outer walls of the tubes available for functionalization, can make them a better candidate compared with their spherical counterparts [3]. Several approaches towards fabricating hollow magnetic tubes involve techniques such as electrodeposition and atomic layer deposition to coat the walls of porous templates [4a,b,c]. A possible drawback of such techniques is the incapability of fabricating single isolated magnetic particles in a controlled fashion, as the common path is to fabricate an array of structures embedded within a porous membrane and to later collect them from a suspension by filtering or drying processes [4a,b,c]. In the past years, a novel approach to build precise tubular structures, combining top–down and bottom–up techniques, has been developed by exploiting the release of pre-stressed thin films to fabricate rolled-up micro- and nanotubes [5, 6]. A variety of exciting applications have been investigated mainly with semiconductors grown by molecular beam epitaxy (MBE) including optical ring resonators [7a,b], microtube integration for fluidic applications [8] and curved electron transport devices [9a,b]. Using semiconductor layers as templates, rolled-up magnetic tubes have been fabricated [10] and characterized [11a,b]. Recently, a new method developed in our group has broadened the range of thin film material systems, including magnetic films, which can be

[4] Author to whom any correspondence should be addressed.

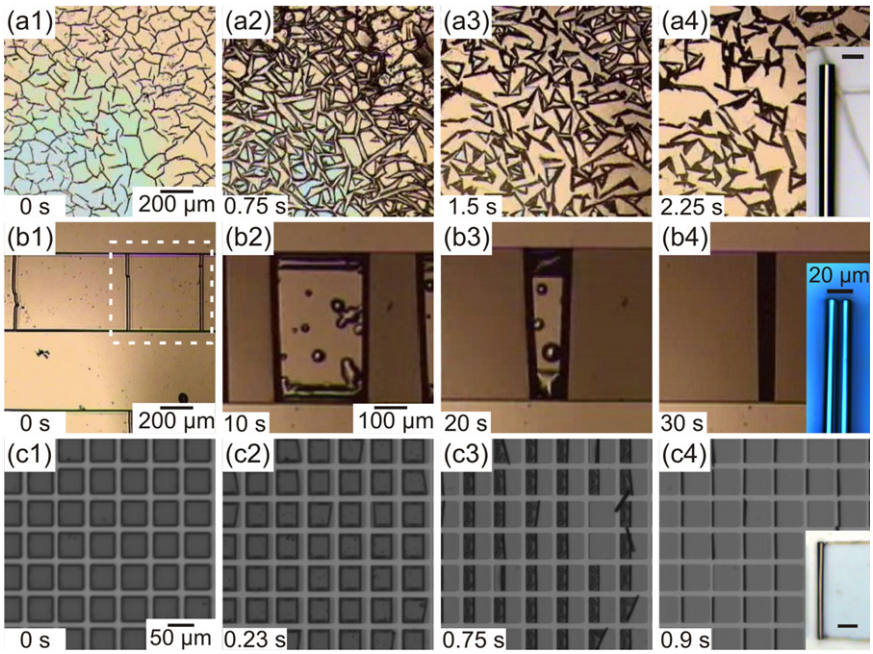

Figure 1. Panels of selected video microscopy images from *in situ* formation observations for three approaches of rolling up magnetic films into microtubes. (*a*1)–(*a*4) Rolling sequence from a Pd/Fe/Pd film with extensive crack formation. The inset in (*a*4) is an optical microscopy image of a single roll with 14 μm in diameter. The scale bar is 20 μm. (*b*1)–(*b*4) Rolling sequence for the same layered system deposited onto a stripe patterned resist, exhibiting a more ordered crack formation. An optical microscopy image of a twin tube structure rolled from the parallel cracks is shown as an inset in (*b*4). (*c*1)–(*c*4) Sequence recorded with a high-speed camera for an array of rolled-up Pd/$Ni_{80}Fe_{20}$/Pd 50 × 50 μm^2 square features, where an angled deposition was used to promote the unidirectional rolling. In the inset of (*c*4) we show an image from a representative microtube from the ensemble, with a diameter of 3 μm. The scale bar is 10 μm.

rolled into tubular structures, and which might be employed as remotely controlled microjet engines in fluids [12].

In this work we present the approach taken towards a deterministic fabrication of ferromagnetic rolled-up microtubes and investigations of their nonlinear rotational dynamics. Magnetic films are released by dissolving an underlying photoresist sacrificial layer, allowing them to release their internal stresses and to self-assemble into tubular structures. Thin films of magnetically soft Permalloy ($Ni_{80}Fe_{20}$) as well as Co/Pt multilayers with typical out-of-plane magnetic anisotropy were successfully rolled into microtubes. The length of the tubes is predefined by lithography while their diameter is shown to scale with thickness. By varying the thickness of the deposited film, tubular structures with a diameter as small as 1.5 μm were achieved. Our studies of the nonlinear rotational dynamics for various lengths of tubes show sensitivities to viscosity variations and suggest that rolled-up technology might be beneficial for the development of new types of multifunctional magnetic sensors on fluids.

2. Results and discussion

2.1. From random to deterministic fabrication

In figure 1, we illustrate through a panel of selected video microscopy images the approach taken towards the fabrication of well ordered ferromagnetic microtube structures by implementing photoresist as the sacrificial layer in the roll-up process. The resist layers can be etched or dissolved with common organic solutions typically used in lift-off processes. Figures 1(*a*1)–(*a*4) show the rolling up sequence of a cracked Pd(5 nm)/Fe(90 nm)/Pd(5 nm) film which was deposited onto an un-patterned resist layer. The Pd layers were introduced as an oxidation protective layer. In this simplest approach, the extensive crack pattern implies that the film has a high built-in average tensile stress [13], and the fractures into the thickness of the layer become narrow slits for the solvent to penetrate, undercut and release the magnetic film. As there is no predefined shape or preference of the underetching front, the film mainly rolled up into random shaped structures, but occasionally into a uniform single tube, as the one shown in the inset of figure 1(*a*4), with a diameter of 14 μm and extending to a length of 255 μm.

As a next step the resist layer was patterned into long stripe features by means of photolithography. We deposited the same layer sequence and observed that the constraint of the film in one of the lateral dimensions promoted a more ordered crack formation in the film perpendicular to the long side of the stripes. Such cracks represent preferred etching windows for the roll-up process, as the film covers the resist side and to a certain extent prevents the film from releasing and rolling up from those points. In figures 1(*b*1)–(*b*4) one can see after the introduction of the solvent how the film rolls up from both cracks towards the centre of the image forming a twin tube structure [14], as the one shown as an inset in figure 1(*b*4), with diameters of ∼10 μm for each tube. A slight buckling of the film propagating towards the centre of the image can be observed in figures 1(*b*2) and (*b*3) due to underetching from

the sides, but the film does not roll up due to the partial coating of the resist side edge.

The last and most refined method comprises an extension of the abovementioned approach, along with the introduction of a special deposition configuration [12]. First we constrict the pattern size in two lateral dimensions by patterning the resist underlayer with feature lengths that are below the crack formation wavelength [13]. Secondly, we deposit the films at an angle with respect to the normal incidence of the material vapour flux. This additional modification has two functionalities. Due to the incident flux, one side of the photoresist edge profile is shadowed and becomes the preferred etching window for the later roll-up process, while the edge to which the deposition is directed at, experiences a rather conformal deposition of the material and becomes the pinning side, which helps the film to roll up into a predefined position on the substrate.

Figures 1(*c*1)–(*c*4) are selected video microscopy images taken with a high-speed camera of the rolling sequence from a Pd(2 nm)/$Ni_{80}Fe_{20}$ (8 nm)/Pd(2 nm) trilayer fabricated with the vapour flux at an angle of $\sim 70^{\circ}$ with respect to the normal incidence. The images illustrate the roll-up process of an array of $50 \times 50\ \mu m^2$ square features rolling together from right to left. In figure 1(*c*4) the final product is a well ordered array of single rolled-up magnetic tubes, although there are structures that have detached from the substrate, which we associate with possible imperfections at the pinning edge of the resist layer. The inset in figure 1(*c*4) is an exemplary rolled-up tube from the ensemble, with a diameter of 3 μm.

The type of rolling process in thin solid films is determined by the built-in strain gradients across the layer thickness, and can be either a roll-up or a roll-down (or inverted roll-up) process, depending on the sign and direction of the strain gradient [15].

Both types of mechanisms have been successfully realized in this work for two different magnetic layered systems. Figure 2(*a*) shows a scanning electron microscopy (SEM) image of a representative microtube 4.6 μm in diameter, which rolled up from a circular pattern of a Pd/$Ni_{80}Fe_{20}$/Pd trilayer system. As an inset we show a schematic illustration of the roll-up process observed for this magnetic film system. The film was deposited in an electron beam evaporator using the refined approach presented earlier and where upon the introduction of the etchant/solvent, the film spontaneously rolls up towards the edge to which the deposition was directed.

The other type of rolling (roll-down) is presented in figure 2(*b*). The inset illustrates the roll-down process observed for a Co/Pt multilayered system, known for perpendicular magnetic anisotropy [16]. A Pt(1 nm)/[Pt(0.8 nm)/Co(0.3 nm)]$\times$8/Pt(5 nm) multilayer stack was evaporated in an MBE chamber, operating at a base pressure of 2×10^{-10} mbar, with deposition rates below 0.1 Å s^{-1}. The deposition was carried out with the vapour flux at normal incidence, as opposed to the angled deposition implemented in the previous layered system. For this type of film we observed *in situ*, during the etching process under an optical microscope, that the film did not roll up but instead buckled upon the introduction of the solvent, suggesting a preference to roll down. Due to the conformal coverage of the film at the edges of the resist, the buckled

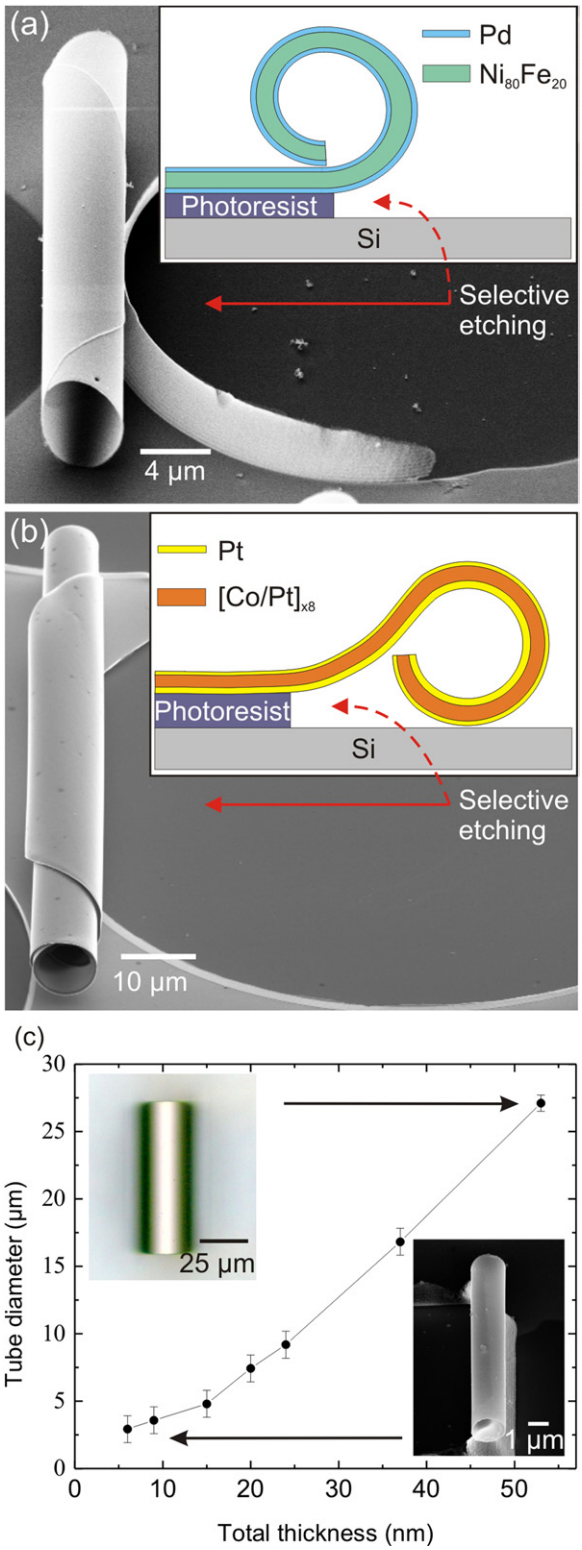

Figure 2. Roll-up and roll-down examples of ferromagnetic microtubes. (*a*) Shows an SEM image of a tube with a diameter of 4.6 μm rolled from a circular pattern of a Pd/$Ni_{80}Fe_{20}$/Pd layered system, the inset is a sketch illustrating the roll-up configuration. (*b*) SEM image from a 8.5 μm diameter tube obtained for the Co/Pt multilayers and also rolled from a circular pattern. The corresponding roll-down configuration is illustrated as an inset. (*c*) Plot of tube diameter as a function of total thickness for a series of Pd/$Ni_{80}Fe_{20}$/Pd samples. The top-left inset shows an optical microscopy image of a 25 μm diameter tube, while the bottom-right inset shows an SEM image from a 1.5 μm tube.

film remained pinned to the edges of the pattern. We assisted the roll-down process by releasing, still in the fluid, the buckled films from one edge using the sharp tip of a glass microcapillary. Upon pinching the film from one of the edges, it rapidly rolled down to shape itself into a tube. Figure 2(*b*) shows an SEM image of a tube, 8.5 μm in diameter, rolled up by this procedure. Since both microtubes shown in figures 2(*a*) and (*b*) were rolled from circular patterns, one can identify the type of rolling experienced by the films by simply looking at the edge feature running along the tube length.

Tuning the diameter of rolled-up polycrystalline films becomes more challenging compared with semiconductor epitaxial layers. The strain gradients that arise from the lattice mismatch of crystalline films can be well determined and used to scale the diameter of the tubes in agreement with theoretical predictions [17a,b]. For metal films, on the other hand, the thermal interactions of the film with the resist layer and the substrate as well as the grain size of the film will influence the value of the residual stress and the potential strain gradients generated across the layer thickness [13]. Two of the most important parameters that influence this in vapour deposited films are the substrate temperature and the growth rate [13]. In figure 2(*c*) we show results of the scalability of the tube diameter as a function of total layer thickness for the Pd/$Ni_{80}Fe_{20}$/Pd system. Samples were grown at room temperature with growth rates of $\sim$0.5 Å s^{-1} for Pd and $\sim$4 Å s^{-1} for the $Ni_{80}Fe_{20}$ layers. Deposition was performed under an angle of 70° and the thickness reported already accounts for the change in the film thickness that arises from the angled deposition [18]. The insets correspond to optical and SEM images from representative tubes with the largest (top-left) and smallest (bottom-right) diameters obtained, $\sim$25 μm and $\sim$1.5 μm, respectively. Such scalability becomes very useful to calibrate fixed parameters for an accurate structure design, and further tuning of the substrate temperature, cooling rates and deposition fluxes can lead to a downsizing of the tube diameters.

2.2. *Nonlinear rotational dynamics of ferromagnetic rolled-up microtubes*

A potential application of the rolled-up microtubes explored in this work relies on the rotational dynamics exhibited by externally driven particles on the micro- and nanoscale, where viscous forces govern over the inertial ones due to the low-Reynolds number (*Re*) environments [19]. The behaviours have been theoretically described [20a,b,c] and studied for a variety of systems, ranging from magnetic holes [20c], paramagnetic particle chains [21], Ni nanowires [22], half-shell magnetic microspheres [23], magnetotactic bacteria [24] and filled carbon nanotubes [25], to optical systems where borosilicate glass nanorods were optically torqued [26].

Ferromagnetic rolled-up microtubes promise to be good candidates for such investigations [12], as the roll-up technique allows us to fabricate samples with well positioned tubes in predefined areas of a substrate and with good tube-to-tube uniformity; hence a number of tubes can be used for calibration measurements and the rest of the ensemble be employed to test

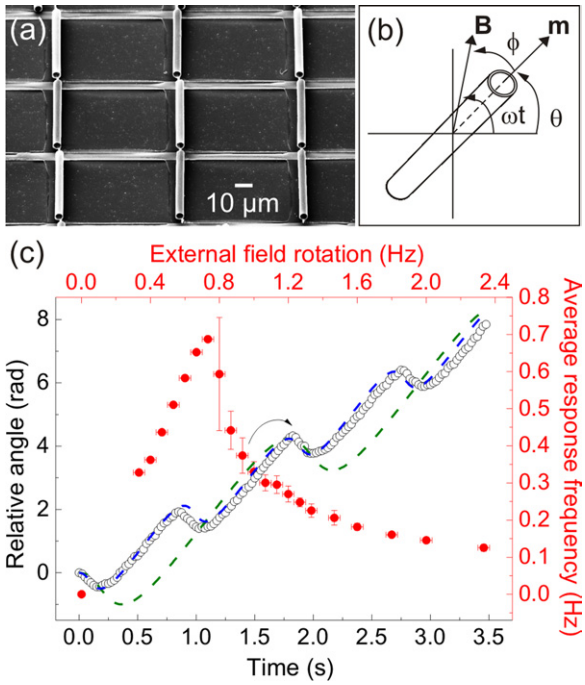

Figure 3. (*a*) An SEM image of an array of $Ni_{80}Fe_{20}$ microtubes with lengths and diameters of 60 μm and 4.5 μm, respectively. (*b*) Schematic of the magnetic rotation geometry. (*c*) A plot of the average response frequency as a function of the external field rotation rate (red solid circles), averaged over three 50 μm long tubes, and the angle variation as a function of time for one of the tubes in a point of the nonlinear regime denoted by the arrow; experimental (black open circles), fittings for case I (lower green dashed curve) and case II (upper blue dashed curve) are shown. (Colour online.)

the fluid or environment of interest. This capability opens the approach for implementing such tubular structures as single probe sensors or carriers in fluidic applications. In figure 3(*a*) we show an SEM image from a close-up view of an array of aligned Permalloy microtubes on a silicon substrate, to illustrate how such structures can be fabricated with good uniformity among them, the diameters were of 4.46 μm with a standard deviation of 0.32 μm and obtained from measuring 64 tubes in the array.

2.2.1. Theoretical description of the rotational motion of micro-nanoparticles at low-Reynolds numbers. At low-Reynolds number environments, inertia contributions can be neglected [19] and the behaviour of a magnetic particle rotating in a viscous medium is determined by the balance between the hydrodynamic or viscous torques (Γ_H) and the magnetic torque (Γ_M) exerted on the particle [20a,b,c]. In figure 3(*b*) we present a sketch of the rotational behaviour for an externally driven microtube, where ωt is the angular variation of the magnetic field $\boldsymbol{B}$, ω being the angular frequency and t the time, θ is the angular orientation of the magnetic moment $\boldsymbol{m}$ with respect to the laboratory frame of view and $\phi = \omega t - \theta$ is the phase lag of the magnetic moment with respect to the field.

The magnitude of the hydrodynamic torque is given by $\Gamma_H = -\gamma(\mathrm{d}\theta/\mathrm{d}t)$, where $\gamma = \kappa V \eta$ is the drag coefficient, κ is the particle shape factor, V is the total volume of the particle

and η is the effective viscosity of the medium. In general, for actively driven particles, two cases have been identified and explored.

Case I. This applies to magnetic particles with constant remanent magnetization M_r, where $m = M_r V_m$ (V_m is the volume of the magnetic material), which are rotated under magnetic fields lower than the coercivity field. The magnetic torque can be written as $|\Gamma_M| = |m \times B|$ and the balance of the torques in the absence of inertia contributions (for our system $Re \approx 10^{-5}$) yields the following equation for the particle motion:

$$\frac{d\phi}{dt} = \omega - \omega_c \sin\phi, \tag{1}$$

where $\omega_c = mB/\gamma$ is the critical frequency of the system.

Depending on the parameter $\alpha = \omega_c/\omega$, this equation has two solutions which describe two regimes of the particle response. If $\alpha > 1$ the particle rotates synchronously with the external field with a constant phase lag given by $\phi = \sin^{-1}(\omega/\omega_c)$. At $\alpha < 1$ the contribution from the viscous torque dominates and overcomes the magnetic torque, which cannot keep up with the external rate, entering a nonlinear regime characterized by back and forth motions, also referred to as flip-backs [26]. The phase lag now becomes a periodic function in time, which, after solving equation (1), can be expressed as

$$\phi = 2\arctan[\alpha + \sqrt{1-\alpha^2}\tan(\sqrt{1-\alpha^2}\omega t/2)]. \tag{2}$$

For $0 \leqslant \phi \leqslant \pi$ the particle moves forward in the direction of the field, while at $\pi \leqslant \phi \leqslant 2\pi$ the sign of the magnetic torque changes and twists the magnetic moment in the opposite direction, giving rise to the backward motion.

Case II. This involves particles in which the dipole moment is induced by the external field, as is the case of a pair of magnetic holes [20c], a paramagnetic particle chain [21] or in optically torqued nanorods [26], but can also account for ferromagnetic particles under applied fields strong enough to affect the magnetization of the particle [20a]. The magnetic torque has the general form of $\Gamma_M = \varepsilon \sin(2\phi)$, where ε is a term proportional to the magnetic content but is also dependent on the particle shape anisotropy [20a,b,c]. This condition leads to an equation of motion as

$$\frac{d\phi}{dt} = \omega - \omega_c' \sin(2\phi), \tag{3}$$

where $\omega_c' = \varepsilon/\gamma$.

At $\omega < \omega_c'$ the phase lag now is $\phi = \frac{1}{2}\sin^{-1}(\omega/\omega_c')$, and in the nonlinear regime the variation in time can be expressed as

$$\phi = \arctan[\alpha' + \sqrt{1-\alpha'^2}\tan(\sqrt{1-\alpha'^2}\omega t/2)] \tag{4}$$

with α' analogous to α.

Note that besides the difference that might arise in the top expression of the critical frequency, the main difference between these two cases is that the maximum phase lag experienced by the particle has a value of $\phi = \pi/2$ for the case of particles with permanent moment under low fields, while for the latter is $\phi = \pi/4$. In turn, this doubles the frequency of flip-backs when the field performs a full rotation around the particle, since the particles with an induced moment or where remagnetization of the particle is feasible, experiences a change in the sign of the magnetic torque at $\phi = \pi/2$, contrary to $\phi = \pi$ as in the permanent moment case.

Interestingly, for both cases, the average rotation rate from the particle can be summarized in the following expression [23, 26]:

$$\langle\dot{\theta}\rangle = \begin{cases} \omega & \omega < \omega_c, \\ \omega - \sqrt{\omega^2 - \omega_c^2} & \omega > \omega_c \end{cases} \tag{5}$$

with the critical frequency having the corresponding value for each case. From this equation one can obtain the following expression to estimate the critical frequency of a system [27]:

$$\omega_c = \langle\dot{\theta}\rangle^{1/2}(2\omega - \langle\dot{\theta}\rangle)^{1/2}. \tag{6}$$

2.2.2. Experimental results of the rotational dynamics from magnetic microtubes at low-Reynolds numbers. To study the rotational dynamics from the magnetic microtubes, we have used tubes rolled up from a $Pd/Ni_{80}Fe_{20}/Pd$ trilayer, with a $Ni_{80}Fe_{20}$ thickness of about 10 nm. For manipulation, glass microcapillaries with needle-like tips and a stage suitable for micromanipulation in an optical microscope were implemented to transfer single microtubes from arrays on a substrate, onto fluid droplets. The tubes were placed onto glycerol/water mixtures and were externally rotated by using a conventional hot plate stirrer, which can apply rates from 0.33 up to 21.66 Hz. The amplitude of the magnetic field exerted by the permanent magnet at the sample position was of ~15 mT. For the analysis, we recorded the motion through a high-speed camera built in an optical microscope.

In figure 3(*c*) we show the results from three 50 μm long microtubes with 4.5 μm diameters rotating on the surface of a 99% glycerol droplet. Image sequences were acquired for external frequencies up to 2.33 Hz, from which the tubes' average rotation response was extracted. The red plot shows the result of averaging the responses over all the tubes and where an average critical frequency of 0.75 ± 0.01 Hz was obtained by using equation (6) and averaging over all points in the nonlinear regime and over the three tubes. The large error bar for the data point at 0.8 Hz can be explained by the fact that at this frequency we observed that two of the tubes had already made the transition into the nonlinear regime, while the other was still rotating synchronously with the external field.

To determine which case of rotational behaviour we are working with, a detailed analysis of the angle variation over time is required. Figure 3(*c*) shows in black open symbols the results of following the angular orientation for one of the 50 μm long tubes, driven at a frequency of 0.93 Hz in the nonlinear regime, corresponding to the point in the solid red plot indicated by the arrow. The lower green dashed curve represents the numerical solution to equation (2) and upper blue dashed curve is that to equation (4), where the parameters of the applied external frequency and the calculated critical frequency from equation (6) were introduced. All the plots were initialized at points before a backward motion occurred in order

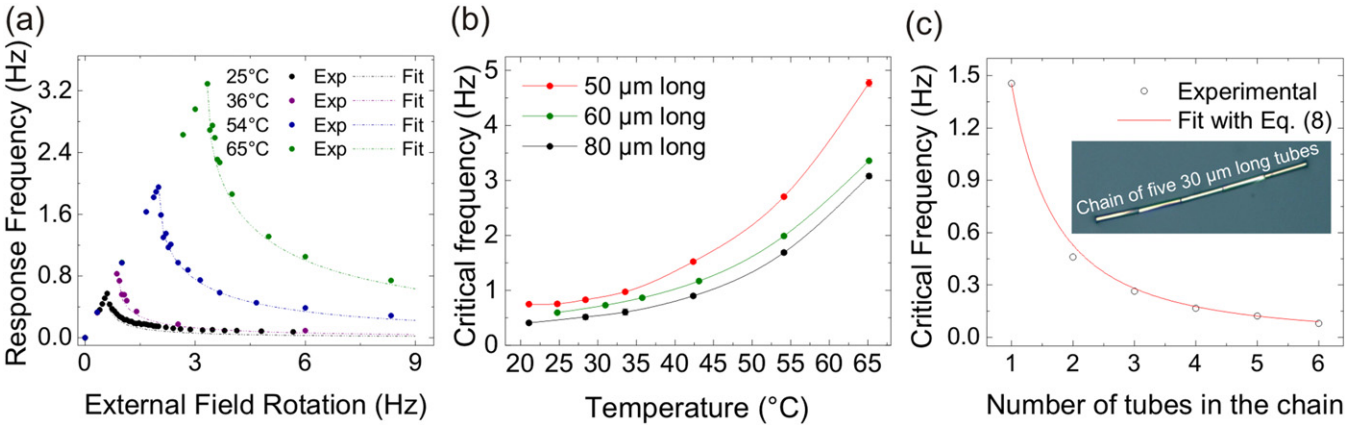

Figure 4. (*a*) Plots of the average responses from a 60 μm long $Ni_{80}Fe_{20}$ microtube for different glycerol temperatures. (*b*) Plots of the variation of the critical frequency as a function of glycerol temperature for tubes with diameter of 4.5 μm and lengths of 50, 60 and 80 μm. (*c*) Plot of the critical frequency dependence with particle shape factor for chains of 30 μm long tubes. Open symbols are experimental values and the curve is a fit using equation (8). The inset shows an optical microscopy image from a chain of five 30 μm long tubes on top of the glycerol surface.

to make a clear comparison. Good agreement with equation (4) suggests that the microtubes, for such applied magnetic field, undergo switching of the magnetization direction during the rotation. Note that the applied magnetic field is larger than typical coercivity values for $Ni_{80}Fe_{20}$ films [28], and it is worth mentioning that previous to the experiments we did not magnetize the samples in preferential direction. One potential application of following the angular variation of a magnetic tube at different applied fields is to estimate which are the coercivity fields for single particles, i.e. by observing a transition in the frequency of flip-backs with a variation in the applied field amplitudes.

The determination and study of shifts in the critical frequency represent an attractive method to investigate a variety of fluid and particle properties, yielding a large range of functionalities [23]. When implementing the same particle and applied field during an experiment, the critical frequency varies as the drag coefficient changes. The drag experienced by the rotating tube strongly depends on the effective viscosity of the fluid as well as on the shape and volume of the structure. In viscous fluids such as glycerol, one can decrease the viscosity by increasing either the water content or temperature of the fluid [29]. We have varied the temperature of a drop of 99% glycerol and recorded the behaviour from single 4.5 μm diameter tubes with lengths of 50, 60 and 80 μm rotating on the surface of the fluid for frequencies up to 8.3 Hz. In figure 4(*a*) we present the response frequencies of the 60 μm long tube for both the linear and the nonlinear regimes from four selected temperatures up to 65 °C. The dashed curves are the fits of the experimental data using equation (5). The shift of the critical frequency towards higher values with increasing temperature is in accordance with a decrease in the fluid effective viscosity. Note that the tubes are rotating on the surface of the liquid, so the viscosity felt is not necessarily just the bulk dynamic viscosity but can include surface effects [22]. After extracting the critical frequencies for this temperature range for the three lengths of rolled-up tubes, we show in figure 4(*b*) that they all follow a comparable trend for the critical frequency variation. The capability of detecting such changes in the fluid properties with different sizes of particles and combined with the design freedom that the rolled-up technology renders on the tubes dimensions, makes them ideal single probe sensors that can satisfy not only a wide range of viscosities but also convenient working parameters. For low viscosities such as in a glycerol solution at room temperature, one can employ a short and narrow microtube. As the viscosity decreases and the critical frequency acquires high working values for the applied external rate, one can use a longer tube with a lower working critical frequency, and in turn the measurement becomes more convenient regarding the external rates and recording rates needed. Another potential application of the magnetic microtubes is to use them as micromixers, where one just needs to design the tubes to have a high value of the critical frequency to allow mixing over a wide range of frequencies.

Further investigations of the parameters affecting the value of the critical frequency rely on the determination and potential calibration of the particles shape, which to a great extent influences the drag coefficient. An interesting approach to investigate mainly the changes due to particle shape and trying to keep every other parameter constant is to take advantage of the magnetostatic interaction that magnetic particles exhibit. We have found that by approaching the tubes on the surface of the viscous liquid, they can interact as small dipole particles and join to form long and stable chains of tubes. This observation also provides a good insight into the remanent state of these structures, with preference of magnetization along the tube axis. By joining almost equal tubes one increases the volume of the particle in the same ratio as the volume of magnetic content, meaning that the contribution from the increment in both parameters cancels out and the main parameter affecting the value of the critical frequency is the shape factor. One could also employ tubes with different lengths for this type of study, as in figure 4(*b*), but the differences that arise in the diameter of the tubes increase the parameters affecting the value of ω_c that have to be taken into account. It is also worth mentioning that as the aspect ratios of the predefined pattern is increased, a highly uniform tube becomes harder to obtain.

In figure 4(*c*) we present the results of the variation of the critical frequency for chains of 30 μm long tubes rotating on the surface of a 95% glycerol/water mixture droplet. We started with a single tube from which a reference critical frequency of 1.45 Hz was measured. Sequentially we added tubes to the chain and measured the critical frequency of the system, and incrementing the chain up to six tubes. For illustration, we show as an inset in figure 4(*c*) an optical microscopy image of a chain with five 30 μm long tubes on top of the liquid surface. The chain formed was observed to be rigid and stable during the whole experiment.

As the microtubes rotate on the surface of the liquid, and to compare with theoretical expressions for the shape factor, we have assumed the tubes to behave as rod-like particles, as we did not observe any fluid entering the tubes. For rod-like particles with an aspect ratio of $p = L/D$, where L and D are the length and the diameter of the particle, respectively, the shape factor from the rotational drag coefficient expression $\gamma = \kappa V \eta$, can be written as [30]

$$\kappa = \tfrac{4}{3} p^2 (\ln p - 0.662 + 0.917/p - 0.05/p^2)^{-1}. \quad (7)$$

Then by taking the critical frequency of the single tube as a reference (ω_c^S), and as long as the applied field and viscosity of the fluid are kept constant, one can make an approximation of the variation of the critical frequency of the chain (ω_c^N) by using the following relation:

$$\omega_c^N = \lambda \frac{\kappa^1}{\kappa^N} \omega_c^S, \quad (8)$$

where κ^N is the shape factor for the chain of N tubes and λ represents a ratio that depends on how the terms in ε will be affected, apart from the content of magnetic material and magnitude of the applied field.

The red curve in figure 4(*c*) is the result of fitting equation (8) for increments in the length of the chain, as the diameter is assumed to stay constant. Good agreement of the experimental data with the estimated variation gives us the confidence to use such expressions to estimate values for shape factors of rolled-up microtubes in future studies.

3. Conclusions

In this work we have described in detail the approach taken towards a deterministic approach for fabricating ferromagnetic rolled-up microtubes. The main approach consists of angle depositing magnetic films by electron beam evaporation onto patterned photoresist layers. These are later dissolved or etched by common organic solvents, allowing the films to release internal stresses and self-assemble into tubular structures. Exemplary results were presented on rolled-up structures evolving from typical soft magnetic films such as Fe and $Ni_{80}Fe_{20}$, to more elaborated systems as Co/Pt multilayered stacks with perpendicular magnetic anisotropy. Other exciting systems of magnetic films should not be limited by these examples, as the main requirement of the rolled-up technique is for the films to exhibit strain gradients across the layers, and the extensive possibilities to combine materials in vapour deposited techniques is vast. Potential use of rolled-up microtubes in fluidic applications was explored by studying the nonlinear rotational dynamics which they exhibit when torqued magnetically in a viscous fluid. We demonstrated sensitivity to viscosity changes for different lengths of tubes, and dependence of the critical frequency on the shape of the particles. The versatility of the technique and the results exposed make the rolled-up microtubes ideal candidates for use as single probe sensors or micromixers, which can be produced accurately on the surface of a substrate and later be transferred individually into the fluid of interest. Finally we expect the rolled-up ferromagnetic microtubes to become a good candidate for research in not only fluidic sensing, but also for understanding their magnetic properties as novel applications that might arise in magneto-electrical sensor devices by exploiting this special cylindrical geometry in thin magnetic films.

Acknowledgments

The authors acknowledge Dr Jens Ingolf Mönch and Sandra Sieber for support in the lithography mask fabrication, Ronny Engelhard and Dominic J Thurmer for experimental assistance and Peter Cendula for fruitful discussions. EBU acknowledges MICIT and CONICIT of Costa Rica for financial support. This work was funded by the BMBF (No 03X5518) Project.

Appendix: Experimental procedures

Photoresist coating and patterning. Silicon wafers were first baked at 120 °C for 10 min to reduce humidity at the surface. An optional step before spin coating the resist but recommended when working with Si or glass substrates was to spin coat TI-Prime from Microchemicals GmbH at 3000 rpm for 20 s, and then a short bake at 120 °C for 2 min. This step promotes a better adhesion of the resist layer to the substrate. Next the ARP-3510 positive resist from Allresist GmbH is spin coated at 3500 rpm for 35 s with a subsequent softbake for 1 min at 95 °C in a hotplate. To pattern the resist we used a Karl Suss MA-56 aligner. The samples were exposed under UV irradiation for 7 s, where specially designed lithography masks with stripes, squares and circles of different dimensions were used. After exposure the resist is developed with a 1 : 1 solution of AR 300-35 developer from MicroChemicals GmbH for 40–60 s to finally obtain the desired pattern in the substrate.

Magnetic thin films preparation. All the layers presented in this work were deposited by electron beam evaporation onto the photoresist layers. Except for the Co/Pt multilayers, the films were deposited in a high vacuum chamber with a base pressure of 8×10^{-8} mbar at room temperature. The films in panels (*a*) and (*b*) from figure 1 were deposited at normal incidence, while all the other films in this work were fabricated with the refined method introduced in figure 1(*c*), they were angled deposited by using specially designed sample holders with planes tilted at 70° with respect to the normal incidence of the vapour flux. Common deposition rates were 2–4 Å s^{-1} for the Fe and $Ni_{80}Fe_{20}$, and 0.5–1 Å s^{-1} for the protective Pd layers. The Co/Pt multilayers were deposited at normal incidence in an MBE chamber with a base pressure of 2×10^{-10} mbar and with deposition rates below 0.1 Å s^{-1} for both materials.

Thin film roll-up process. The prepared samples with metal films onto photoresist were rolled up by using organic solvents to dissolve away the resist layer, and letting the film release and roll up into a tube. The main solvent used was acetone, but other organic solvents such as ethanol or isopropanol can also selectively dissolve the resist without damaging the layers. An optional step before drying the samples but which we highly recommend when working with very thin layers is to perform a supercritical drying step in order to avoid collapse of the structure due to strong capillary forces. For this we have used a Critical Point Dryer, model CPD 030 from Bal-Tec AG. This drying step keeps the tubes from collapsing since a continuous density change from liquid to gas is performed and thus eliminates problems due to surface tensions.

In situ observation of the roll-up process and microtube characterization. Video microscopy observations were performed in an optical microscope (Zeiss VMG 160) for the images in panels (*a*) and (*b*) in figure 1, and in an optical microscope (Zeiss Axiotech vario) with incorporated high-speed camera (Photonic Science Limited) for panel (*c*) in figure 1. The rolled-up microtubes were characterized in an optical microscope (Zeiss Axiotech vario) and by SEM (Zeiss NVision 40).

Studies of the rotational dynamics. Single microtubes were picked up from the substrate by using sharp glass microcapillaries. The microcapillaries were obtained in a NARISHIGE PC-10, where sharp needle-like tips can be fabricated. Using a micromanipulator installed in the optical microscope we approached the microtubes in the substrate with the microcapillary, picked them up (the tubes attach easily upon contact with the capillary due to electrostatic interactions) and transfered them into droplets of glycerol (99.5% Merck)–water mixtures placed on top of a microscope glass slide.

To apply the rotating external magnetic field we used a Heidolph MR-3004 safety hot plate stirrer which can apply rotating rates from 20 to 1500 rpm in steps of 4 rpm and can also vary the temperature of the plate. The microscope glass slide was positioned in the middle of the plate and the amplitude of the magnetic field measured at this point was 15 mT. The rotational dynamics were studied with the already mentioned high-speed camera in the optical microscope. The recorded images were analysed using the 'ImageJ' software from the National Institutes of Health (NIH).

References

[1] Wiltshire M C K, Pendry J B, Young I R, Larkman D J, Gilderdale D J and Hajnal J V 2001 *Science* **291** 849

[2] (a) Kläui M, Rothman J, Lopez-Diaz L, Vaz C A F, Bland J A C and Cui Z 2001 *Appl. Phys. Lett.* **78** 3268
(b)Albrecht M, Hu G, Guhr I L, Ulbrich T C, Boneberg J, Leiderer P and Schatz G 2005 *Nature Mater.* **4** 203

[3] Son S J, Reichel J, He B, Schuchman M and Lee S B 2005 *J. Am. Chem. Soc.* **127** 7316

[4a] Bao J, Tie C, Xu Z, Zhou Q, Shen D and Ma Q 2001 *Adv. Mater.* **13** 1631

[4b] Daub M, Knez M, Goesele U and Nielsch K 2007 *J. Appl. Phys.* **101** 09J111

[4c] Bachmann J, Jing J, Knez M, Barth S, Shen H, Mathur S, Goesele U and Nielsch K 2007 *J. Am. Chem. Soc.* **129** 9554

[5] Schmidt O G and Eberl K 2001 *Nature (London)* **410** 168

[6] Prinz V Y, Seleznev V A, Gutakovsky A K, Chehovskiy A V, Preobrazhenskii V V, Putyato M A and Gavrilova T A 2000 *Physica E (Amsterdam)* **6** 828

[7a] Songmuang R, Rastelli A, Mendach S and Schmidt O G 2007 *Appl. Phys. Lett.* **90** 091905

[7b] Kipp T, Welsch H, Strelow Ch, Heyn Ch and Heitmann D 2006 *Phys. Rev. Lett.* **96** 077403

[8] Thurmer D J, Deneke Ch, Mei Y F and Schmidt O G 2006 *Appl. Phys. Lett.* **89** 223507

[9a] Mendach S, Schumacher O, Welsch H, Heyn Ch, Hansen W and Holz M 2006 *Appl. Phys. Lett.* **88** 212113

[9b] Shaji N, Qin H, Blick R H, Klein L J, Deneke Ch and Schmidt O G 2007 *Appl. Phys. Lett.* **90** 042101

[10] Deneke Ch, Schumann J, Engelhard R, Thomas J, Sigle W, Zschieschang U, Klauk H, Chuvilin A and Schmidt O G 2008 *Phys. Status Solidi* c **5** 2704

[11a] Deneke Ch, Schumann J, Engelhard R, Thomas J, Müller C, Khatri M S, Malachias A, Weisser M, Metzger T H and Schmidt O G 2009 *Nanotechnology* **20** 045703

[11b] Mendach S, Podbielski J, Topp J, Hansen W and Heitmann D 2008 *Appl. Phys. Lett.* **93** 262501

[12] Mei Y F, Huang G S, Solovev A A, Bermúdez Ureña E, Mönch J I, Ding F, Reindl T, Fu R K Y, Chu P K and Schmidt O G 2008 *Adv. Mat.* **20** 4085

[13] Freund L B and Suresh S 2003 *Thin Film Materials* (Cambridge: Cambridge University Press) chapters 2 and 4

[14] Schmidt O G, Deneke Ch, Kiravittaya S, Songmuang R, Heidemeyer H, Nakamura Y, Zapf-Gottwick R, Müller C and Jin-Phillipp N Y 2002 *IEEE J. Sel. Top. Quantum Electron.* **8** 1025

[15] Songmuang R, Deneke Ch and Schmidt O G 2006 *Appl. Phys. Lett.* **89** 223109

[16] Suzuki T 1995 *Scr. Metall. Mater.* **33** 1609

[17a] Deneke Ch, Müller C, Jin-Phillipp N Y and Schmidt O G 2002 *Semicond. Sci. Technol.* **17** 1278

[17b] Zang J and Liu F 2008 *Appl. Phys. Lett.* **92** 021905

[18] Robbie K, Beydaghyan G, Brown T, Dean C, Adams J and Buzea C 2004 *Rev. Sci. Instrum.* **75** 1089

[19] Purcell E M 1977 *Am. J. Phys.* **45** 3

[20a] Newman J J and Yarbrough R B 1968 *J. Appl. Phys.* **39** 5566

[20b] Valberg P A and Butler J P 1987 *Biophys. J.* **52** 537

[20c] Helgesen G, Pieranski P and Skjeltorp A T 1990 *Phys. Rev. Lett.* **64** 1425

[21] Biswal S L and Gast A P 2004 *Phys. Rev.* E **69** 041406

[22] Anguelouch A, Leheny R L and Reich D H 2006 *Appl. Phys. Lett.* **89** 111914

[23] McNaughton B H, Kehbein K A, Anker J N and Kopelman R 2006 *J. Phys. Chem.* B **110** 18958

[24] Ērglis K, Wen Q, Ose V, Zeltnis A, Sharipo A, Janmey P A and Cēbers A 2007 *Biophys. J.* **93** 1402

[25] Korneva G, Ye H, Gogotsi Y, Halverson D, Friedman G, Bradley J and Kornev K G 2005 *Nano Lett.* **5** 879

[26] Shelton W A, Bonin K D and Walker T G 2005 *Phys. Rev.* E **71** 036204

[27] McNaughton B H, Agayan R R, Wang J X and Kopelman R 2007 *Sensors Actuators* B **121** 330

[28] Akhter M A, Mapps D J, Ma Tan Y Q, Petford-Long A and Doole R 1997 *J. Appl. Phys.* **81** 4122

[29] Shankar P N and Kumar M 1994 *Proc. R. Soc. Lond.* A **444** 573

[30] Tirado M M and García de la Torre J 1993 *J. Chem. Phys.* **73** 1993